Available online at www.sciencedirect.com
ScienceDirect
Catalysis Today 130 (2008) 24–31
CATALYSIS TODAY
www.elsevier.com/locate/cattod

Solution synthesis of the unsupported Ni–W sulfide hydrotreating catalysts

Zhang Le [a], Pavel Afanasiev [b,*], Dadong Li [a], Xiangyun Long [a], Michel Vrinat [b]

[a] *Research Institute of Petroleum Processing, SINOPEC, 18 Xue Yuan Road, 100083 Beijing, PR China*
[b] *Institut de Recherches sur la Catalyse, 2 Avenue A. Einstein, 69626 Villeurbanne Cédex, France*

Available online 20 August 2007

Abstract

Three solution synthesis routes for the preparation of unsupported Ni–W–S hydrotreating catalysts were compared. In all of them $WO_2S_2^{2-}$ core was applied as precursor, but the reaction between Ni and W species was done in different ways. The preparation methods included solution reaction between $WO_2S_2^{2-}$ and nickel species in the presence of organic surfactant (liquid–liquid route), reaction of amorphous high surface area nickel compound with aqueous $WO_2S_2^{2-}$ species (liquid–solid route) and reaction of amorphous WOS_2 solid with aqueous solution of nickel salt (solid–liquid route). The catalysts were characterized by several techniques including X-ray powder diffraction, specific surface area and pore volume measurements, transmission electron microscopy and X-ray photoelectron spectroscopy (XPS). The catalytic activities were evaluated in thiophene hydrodesulfurization (HDS), toluene hydrogenation (HYD) and pyridine hydrodenitrogenation (HDN) reactions. It has been shown that highly active unsupported sulfides can be obtained from three routes. The highest weight activity was observed for the most finely dispersed liquid–liquid preparation. However, the relation between catalytic activity and texture is not linear and the preparation having low surface area and containing NiS bulky particles covered by curved WS_2 slabs showed the highest activity per unit of surface area.

Keywords: Nickel; Tungsten; Unsupported catalyst; Hydrotreating; Thiosalt; XPS

1. Introduction

In order to protect the urban areas, environmental legislation has been adopted to limit the sulfur level in diesel fuel and the need to produce extremely clean fuel is continually increasing. Conversion of sulfur compounds is therefore of prime importance, and such an objective needs the development of more active catalysts. Usually the hydrodesulfurization (HDS) catalysts contain molybdenum sulfide promoted with cobalt or nickel and supported on a high surface area alumina. Currently, new catalysts appeared on the marked, which contain very high amount of sulfide and can be considered as unsupported systems. The development of such unsupported systems bearing very high density of active sites seems to be a promising research direction [1]. Many works dealt with the preparation of the unsupported molybdenum-based catalysts, see, for instance, Refs. [2–5]. However, the NiW sulfide bulk systems are less studied.

Supported nickel tungsten catalysts have been studied for long time and showed some interesting properties. Yet in 1988 a special issue of *Catal. Today* dealt with the alumina supported NiW catalysts [6]. In these works the most important particularities of the W-based sulfide catalysts were noted such as high hydrogenating power and difficult sulfidation, requiring enhanced temperatures. Later, some works have dealt with the support influence, the effect of dopants and alternative preparation routes. However, compared to molybdenum-based catalysts, the hydrotreating catalysts based on tungsten are relatively less studied [7–24]. The ensemble of previous work suggested that the active phase of supported NiW sulfide catalysts is similar to the Co(Ni)MoS phase in the molybdenum analogs, being attributed to the edge decorated WS_2 slabs by Ni or Co atoms. However, the analogy between molybdenum and tungsten in this type of catalysts often falls short. Thus, contrarily to the CoMoS phase, the corresponding CoW active structure cannot be obtained by sulfidation of oxidic precursors but needs using of alternative preparation approaches [25,26].

* Corresponding author. Tel.: +33 4 72 44 53 39; fax: +33 4 72 44 53 99.
E-mail addresses: afanas@catalyse.univ-lyon1.fr, afanas@catalyse.cnrs.fr (P. Afanasiev).

0920-5861/$ – see front matter © 2007 Elsevier B.V. All rights reserved.
doi:10.1016/j.cattod.2007.07.002

There are quite a few studies on the unsupported NiW systems [27–33]. Lacroix et al. [28] prepared the unsupported catalysts using homogeneous precipitation technique. The solids obtained had moderate specific surface area of 3–20 m^2/g and demonstrated high intrinsic hydrogenation (HYD) activity. Later the unsupported NiW sulfide catalysts were investigated by Fuentes and co-workers and Alonso et al. who carried out syntheses of unsupported Ni/WS_2 catalysts by ex situ and in situ decomposition of thiosalts [29–33]. In these works fully sulfided ammonium or alkylammonium thiotungstates were used as precursors. Contrarily to the consensus existing on the positive role of carbon in the molybdenum-based sulfide catalysts [34] the presence of carbon in the tetraalkylammonium precursors was reported to accelerate the crystallization rate of WS_2-based catalysts leading to low specific surface areas and low activities. Pedraza and Fuentes [32] observed for the NiW sulfides much lower specific and intrinsic activities as compared to the Mo-based counterparts. Overall, the NiW sulfides studied in these works showed some interesting properties, but their activities were almost always compared between the unsupported systems and not with the commercial alumina supported systems. The only comparison with industrial alumina supported NiMo made in Ref. [33] showed that the best unsupported catalyst obtained from thiosalts had HDS activity close to that of the industrial reference.

The aim of this work was to compare different approaches to the preparation of unsupported NiW systems and to evaluate their performance in several model hydrotreating reactions.

2. Experimental

2.1. Preparation of $(NH_4)_2WO_2S_2$ oxothiotungstate (OTT) precursor

Ammonium metatungstate (20 g, ca. 0.1 mol W) was dissolved in 50 ml of concentrated NH_4OH and 40 ml H_2O and stirred for 1 h. Then 100 ml of $(NH_4)_2S$ (50 wt.%) was rapidly added to the solution at ambient temperature. Yellow precipitate was formed which was isolated by filtration and dried under nitrogen flow. It was identified as OTT by XRD and chemical analysis.

2.2. Catalysts preparation

2.2.1. Liquid–liquid technique (solution reaction of tungsten and nickel precursors L_WL_{Ni} solids)

In the liquid–liquid (l–l) technique the unsupported Ni–W pre-catalysts were prepared by solution reaction between OTT and aqueous Ni^{2+}, eventually in the presence of ethylene glycol and organic surfactant. In a typical preparation, to a solution of 2 g (about 0.003 mol) of OTT in 100 ml of distilled water, 100 ml of ethylene glycol, and 30 ml non-ionic surfactant Triton X114, was added 50 ml of aqueous solution containing 1 g (0.003 mol) of $Ni(NO_3)_2{\cdot}6H_2O$. The resulting dark precipitate (pre-catalyst) was separated by centrifugation and dried overnight under vacuum at 80 °C. The black solids produced by solution reaction were sulfidized under 15 vol.% H_2S/H_2 at 400 °C for 4 h.

2.2.2. Liquid–solid route (dissolved tungsten and solid nickel precursors, L_WS_{Ni} solids)

In this route, the catalysts were prepared by reaction of amorphous high surface area nickel basic carbonate compound $Ni(OH)_2{\cdot}NiCO_3{\cdot}H_2O$ with aqueous solution of $(NH_4)_2WO_2S_2$. In a typical preparation, the aqueous suspension of 2 g nickel basic carbonate in 50 ml distilled water was stirred. Then the solution of 4 g of OTT dissolved in 100 ml distilled water was added dropwise. The mixture was kept stirred for 1 h at room temperature. Drying of the filtered precipitate under vacuum and sulfiding under 15% (v) H_2S/H_2 at 400 °C for 4 h produced 1.5 g of a black solid. This synthesis route was called l–s route and the final product is further called L_WS_{Ni}. The l–s route preparations were carried out with different solvents, nickel to tungsten mole ratios and pH values.

2.2.3. Solid–liquid route (solid tungsten and dissolved nickel precursor, S_WL_{Ni} solids)

In this approach prior to the NiWS catalyst synthesis, amorphous tungsten oxosulfide {WOS_2} precursor was obtained by heating of $(NH_4)_2WO_2S_2$ under N_2 or 15% (v) H_2S/H_2 at 423–673 K for 4 h. Alternatively it also could be prepared by acidification of the OTT solution (2 wt.%). In a typical precipitation 100 ml of OTT solution was rapidly mixed with equal volume of 0.1 M HCl. Black precipitate was formed instantaneously with quantitative yield. After collecting, drying under nitrogen flow, WOS_2 solid was obtained. To obtain NiWS unsupported catalyst, 1.6 g of {WOS_2} solid was impregnated with 1 g of nickel nitrate in 1 ml of distilled water for 2 h. The mixture was then dried under vacuum and sulfided under 15% (v) H_2S/H_2 at 400 °C for 4 h. This synthesis route was called s–l route and the final product prepared with this route is called S_WL_{Ni} in the following text. The s–l route was carried out with different tungsten precursors, solvents and sulfiding temperatures.

2.3. Characterizations

The X-ray diffraction patterns were obtained on a Bruker diffractometer with Cu Kα radiation. Standard JCPDS files were employed to identify the phases. Chemical analyses were realized using the atomic emission method with a spectroflame ICPD device. The surface areas and pore volumes were determined by low-temperature nitrogen adsorption using, respectively, the BET and the BJH equations.

For the X-ray photoelectron spectroscopy (XPS) analysis the sulfided samples were transferred into a glove box without air exposure. The samples were pressed on an indium foil attached to the sample holder and transported into the preparation chamber of the XPS machine. The XPS spectra were recorded on a VG Instrument type ESCALAB 200R system. The sample excitation was done by Al K X-rays (1486.6 eV). Peak shifts due to charging of the samples were corrected by taking the C 1s line of carbon residuals at 285.0 eV as a reference.

High-resolution electron microscopy (HREM) examinations were performed with a JEOL 2010 (200 kV) instrument equipped with a Link ISIS micro-analysis system. Its resolution is 0.195 nm. Freshly sulfided catalyst sample was ultrasonically dispersed in an ethanol solution at room temperature and the suspensions were collected on a carbon-coated copper grid. In the sulfided state, W catalysts contain WS_2 stacks. The average number of layers per stack and the average stack length were calculated based on the examination of several hundreds of WS_2 domains.

2.4. Catalytic tests

The catalytic activity tests for thiophene HDS were carried out in a glass micro-reactor in a continuous operating mode and at atmospheric pressure. Appropriate amount (ca. 50–70 mg) of catalyst was used in order to keep the conversion below 20%. The thiophene was introduced into the reactor by flowing H_2 (50 ml/min) through a saturator maintained at 273 K. The reaction was running at 573 K overnight until the conversion became stable, and after being evaluated in the range from 553 to 593 K. The products were analyzed using on-line gas chromatography equipped with a FID detector and a 30 m × 0.53 mm capillary column coated with a homogeneous layer of Al_2O_3 deactivated by Na_2SO_4. The rate of thiophene transformation was calculated as $R_s = (F/m)X$, where R_s is the specific rate expressed as moles of thiophene transformed per second and per gram of catalyst, F is the molar flow rate of reactant, m represents the mass of catalyst and X is the fractional thiophene conversion.

The toluene HYD reaction was performed on a fixed-bed micro-reactor and the reaction products were collected and identified using a gas chromatograph with a capillary column. The reactor was a stainless steel tube with the size of 5.8 mm × 14 mm × 300 mm. The system pressure was adjusted by back-pressure regulator. The feed was input to the system by the ConstaMetric® 4100 liquid pump. Approximately 0.15 g of catalyst was used for the tests and the feed was 8 wt.% toluene dissolved in hexane. The HYD activity was tested at 603 K. The only observed products of toluene reaction were methylhexane and dimethylpentane.

The catalytic activity in the pyridine hydrodenitrogenation (HDN) reaction was tested in the same flow reactor under the almost same conditions as for the toluene HYD. Approximately 0.30 g of catalyst was used. The feed was 10 wt.% pyridine solved in the hexane. The HDN activity was tested at 633 K. The observed products of pyridine reaction were pentane, piperidine and pentylamine.

3. Results and discussion

3.1. Properties of the solids before and after sulfidation

Being assisted by our previous experience on the Mo sulfides [35,36] we developed new synthesis methods targeting preparation of highly dispersed NiW unsupported catalysts. The OTT precursor was applied in all of them, which is much easier to prepare than fully sulfided thiosalt, but provides two sulfurs per one tungsten atom, sufficient to obtain sulfide in a solution reaction or by decomposition. Easier preparation was the main reason of choice of the OTT precursor, whereas thiotungstate was already successfully used to prepare catalysts [29–33]. Note that several experiments we carried out with fully sulfided thiotungstate gave similar results as the OTT-derived catalysts, but they are not included in the present paper.

In the three routes the solids genesis was drastically different. In the liquid–liquid route the co-precipitation of Ni and W species occurred from the homogeneous solutions of molecular precursors. In the l–s route the surface of poorly crystalline basic nickel carbonate reacted with the anions from OTT solution. Finally, in the s–l technique amorphous or poorly crystalline tungsten oxysulfide was impregnated by a nickel salt similarly to the CoMoS synthesis described in Ref. [36]. Amorphous tungsten oxysulfide is an intermediate product of OTT decomposition which is described in detail elsewhere [37].

All these preparations were studied at different reaction conditions and optimized as concerns the textural properties of the products and their catalytic activity. The results of optimization and the influence of various synthesis parameters on the catalysts properties are discussed in Refs. [37,38]. Here we only report on the best catalysts obtained within each of these techniques and compare them with the unsupported individual sulfides and with the well-known commercial supported references. Note only that the optimized techniques l–l and s–l involve the use of non-ionic surfactant and ethylene glycol as the mixed solvent as well as the proper choice of Ni precursor and pH adjust. Unlikely to the molybdenum analogue [36], precipitation of OTT by means of acid, with or without adding of surfactant and glycol, gave low surface areas and poor activity of the corresponding materials. Therefore, s–l preparations considered include only those from the thermal decomposition of OTT. The preparation conditions and the most important properties of the solids obtained are summarized in Table 1. The sulfidation temperature of 673 K was applied. The possible temperature interval of activation seems to be rather narrow, since below 673 K sulfidation was not sufficiently deep and above 723 K progressive sintering occurred.

The XRD patterns (Fig. 1 a) showed that all the pre-catalysts were virtually amorphous regardless the preparation method used. Further sulfidation yielded crystalline phases NiS and WS_2 in the XRD patterns (Fig. 1b). The broad peaks of WS_2 were observed in the XRD patterns of all three sulfide catalysts suggesting that WS_2 is poorly crystallized or exists in a ''rag like structure'' of folded and disordered WS_2 layers as proposed by Chianelli et al. [40]. Among the XRD patterns of the three catalysts, the broadest peaks of WS_2 were observed for the L_WL_{Ni} solid. The width of the (0 0 2) peak allowed calculation of the average stacking of the WS_2 layers. The WS_2 stacking so calculated are 2.05 nm (3 layers), 2.70 nm (4 layers) and 2.44 nm (4 layers) respectively in the sulfided solids S_WL_{Ni}, L_WS_{Ni} and L_WL_{Ni}. The XRD patterns showed the decrease of NiS lines intensity in the sequence $L_WS_{Ni} \gg S_WL_{Ni} > L_WL_{Ni}$

Table 1
Preparation conditions and properties of the sulfide catalysts issued from the three synthesis routes, compared to the references samples

Sulfide solid	Precursors used	r	R	S (m^2/g)	Vp (cm^3/g)	HDS rate (10^{-8}mol/g s)		
						573 K	593 K	613 K
S_WL_{Ni}	WS_2O, $Ni(NO_3)_2$, H_2O, EG, Triton 114	0.37	0.4	58	0.12	289	554	879
L_WS_{Ni}	OTT, $Ni_2CO_3(OH)_2$, H_2O	0.67	0.76	26	0.09	204	336	481
L_WL_{Ni}	OTT, $Ni(NO_3)_2$, H_2O, EG, Triton 114	0.41	0.65	108	0.20	402	667	888
MoS_2	Reference solid	–	–	60		12	21	39
WS_2	Reference solid	–	–	21		9	17	33
NiW/Al_2O_3	Reference catalyst		0.31			187	285	434
$NiMo/Al_2O_3$	Reference catalyst		0.3	200		200	389	577

OTT: Ammonium oxothiotungstate. r = Ni/(Ni + W) mole ratio input to the reaction solution. R = Ni/(Ni + W) mole ratio in the sulfide solid.

In the first one NiS phase gives the most intense reflections while in the last one it can be considered as impurity.

Transmission electron microscopy (Fig. 2) revealed strong differences between the solids prepared via three routes The TEM images of the sulfided S_WL_{Ni} and L_WL_{Ni} catalysts showed only the presence of random WS_2 layer stacks as a unique feature (Fig. 2A, C and D). The L_WL_{Ni} specimen showed the presence of some tubule like objects, which are a common feature for the surfactant-assisted syntheses. Their amount in the L_WL_{Ni} specimen was less than 10% of the total solid volume. Nickel sulfide (even if small peaks were present in the XRD patters) was not found in the samples by TEM study. Within the layers the amount of nickel was close to the value determined by chemical analysis and homogeneously distributed, suggesting the formation of ''Ni–W–S'' phase.

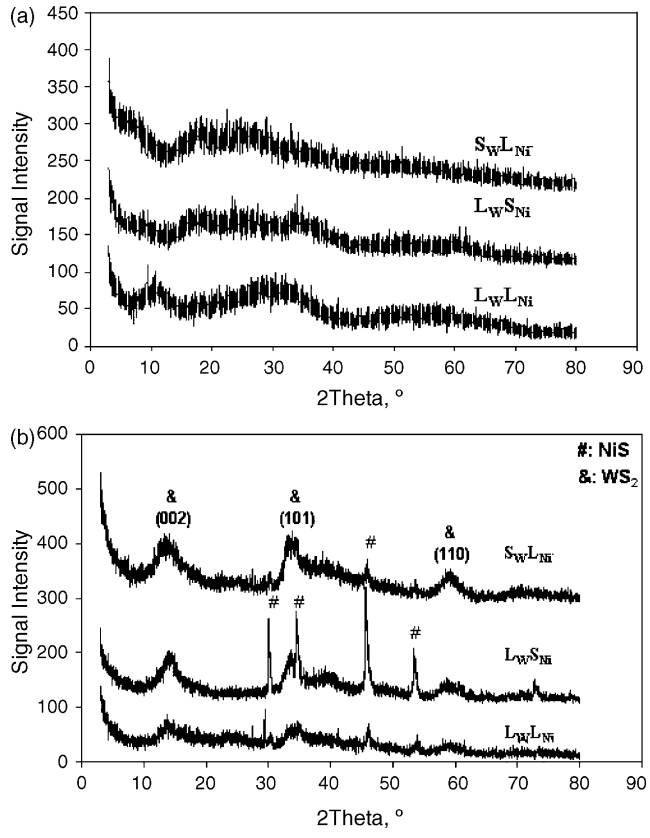

Fig. 1. (a) XRD patterns of the pre-catalysts prepared with different techniques; (b) products of their sulfidation at 673 K.

Entangled WS_2 slabs were rather difficult to analyze statistically since the particles overlapped. However, on the basis of comparison of 300–500 domains in each solid, we found that in the TEM images of S_WL_{Ni} catalyst, the WS_2 stacks were mostly present as 3–4 layers stacks and had the slabs' length was about 6 nm. The WS_2 stacks in the TEM images of L_WL_{Ni} catalyst were slightly more stacked (3–5 layers) and had shorter average length of about 5 nm. The situation was very different for the sulfided L_WS_{Ni} sample. Two different crystalline phases WS_2 and NiS, could be clearly distinguished by TEM. In all images NiS crystals were covered by curved slabs of WS_2 (Fig. 2B). The WS_2 stacks usually had 2–4 layers. The length of the slabs was smeared over a large range from 3 nm to very long (many tens of nm, for the slabs surrounding the particles). Such core shell structures were observed previously by Pedraza and Fuentes in the systems prepared from the decomposition of thiosalts [32]. The results of TEM study are in good agreement with the XRD data. Indeed, in the sulfided catalysts S_WL_{Ni} and L_WL_{Ni}, the NiS phase was minor and could not be observed in the TEM images. By contrast, the NiS peaks were sharp and strong in the diffraction pattern of the sulfide catalyst L_WS_{Ni}.

3.2. Catalytic properties

As can be seen from Table 1, three preparation routes produced sulfide solids with great differences of the properties. All these catalysts possess good activity in thiophene HDS reaction, much higher than the non-promoted molybdenum and tungsten sulfides, and more or less higher than the industrial reference NiW (21% W, 3% Ni on alumina) or NiMo (9% Mo, 3% Ni on alumina) catalysts. The L_WS_{Ni} sample had almost the same HDS activity as the supported reference. The best catalyst L_WL_{Ni} had the specific thiophene HDS activity almost two times higher, the activity of S_WL_{Ni} was intermediate. To our knowledge this is the first report on so highly active NiW bulk catalysts. Note however that the gain of thiophene HDS activity over the supported reference is somewhat smaller for the NiW systems than observed previously for the similarly prepared CoMoS unsupported catalysts [39].

The same sequence of activity as in HDS, the unsupported catalysts under study showed in the toluene HYD and pyridine HDN reactions (Tables 2 and 3). Again the L_WL_{Ni} catalyst had two times higher HDN and HYD activity than the reference.

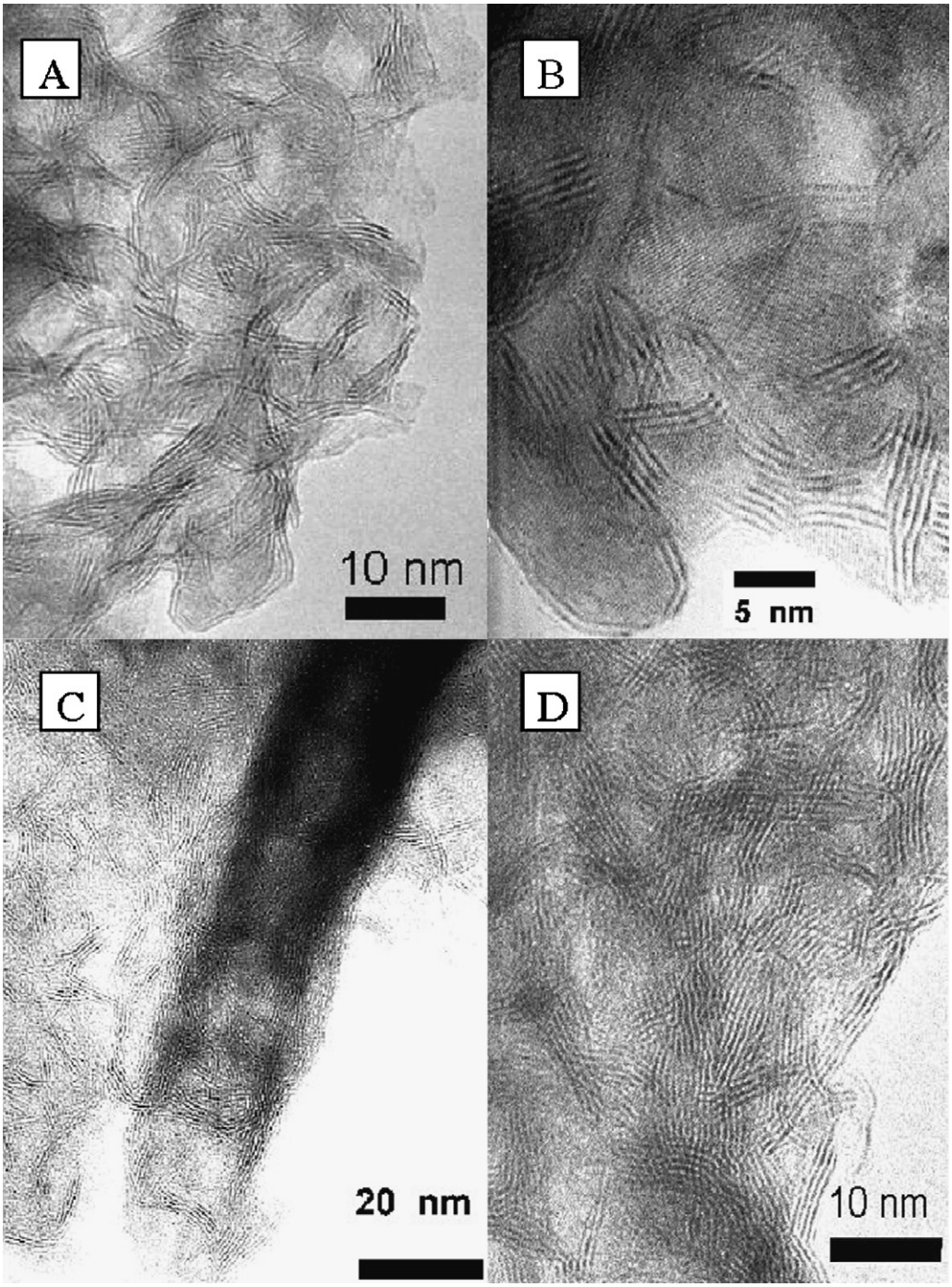

Fig. 2. TEM images of the sulfided catalysts: S_WL_{Ni} (A), L_WS_{Ni} (B) and L_WL_{Ni} (C and D).

Table 2
Catalytic activities for pyridine reaction at 633 K

Catalyst	k_T (10^{-7} mol/s g)	k_{HDN} (10^{-7} mol/s g)
$NiMo/Al_2O_3$	49.77	23.63
L_WL_{Ni}	76.93	50.79
L_WS_{Ni}	35.49	9.35
S_WL_{Ni}	40.43	14.28

k_T is total conversion rate, k_{HDN} is hydrodenitrogenation rate.

Table 3
Catalytic activity for toluene HYD reaction at 603 K

Catalyst	k_{ISOM} (10^{-7} mol/s g)	k_{HYD} (10^{-7} mol/s g)
$NiMo/Al_2O_3$	1.79	61.41
L_WL_{Ni}	2.56	120.34
L_WS_{Ni}	0.75	75.28
S_WL_{Ni}	0.73	41.13

k_{ISOM}: Isomerisation rate, k_{HYD}: hydrogenation rate, see Ref. [22].

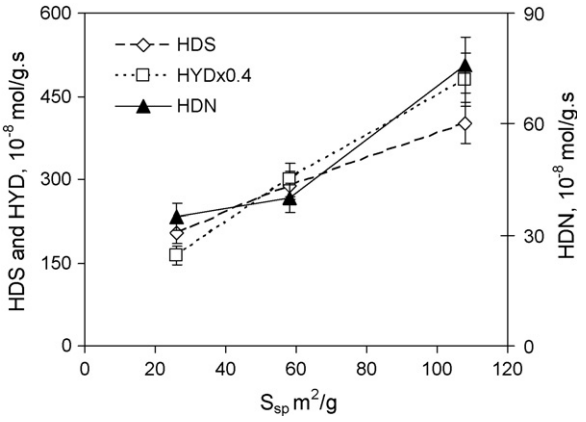

Fig. 3. Correlation between the specific surface area of the Ni–W–S systems studied and their activity in three model reactions.

The L_WS_{Ni} and S_WL_{Ni} catalysts had approximately equal or lower HDN activity than the supported catalyst as they did in the thiophene evaluation. The difference of selectivity (at similar conversion level) should be noted. Only one fourth of the pyridine conversion products is due to HDN for the L_WS_{Ni} specimen, whereas they represent majority in the case of L_WL_{Ni} one. Such a striking selectivity difference correlates with their dissimilar morphology. In any case it is not compatible with the assumption of single type of active centres.

If we consider correlation of the catalytic activity in three reactions to the specific surface area of the solids, it can be noticed that a roughly linear relationship exists, but the formally traced correlation curve certainly does not pass through zero (Fig. 3). The physical meaning of this is that low surface area solid possesses higher intrinsic activity than high surface ones. Though in three reactions the behaviour was somewhat unequal, for all of them the L_WS_{Ni} specimen had the highest activity per unit of surface (but unfortunately it has low surface area). Therefore, when the additional surface area was created, either the relative content of active sites in the solid or their quality was decreased.

This is a surprising finding since the TEM and XPS data (vide infra) suggest the opposite, namely higher relative amount of "NiWS" phase in the L_WL_{Ni} specimen. In the supported catalysts, the Ni to W ratio was reported to have optimal value of R in the range 0.4–0.5 [22]. From our data it follows that Ni-overloaded solid L_WS_{Ni} containing bulky NiS crystals possess twice as higher intrinsic activity in all three reactions studied that better dispersed counterparts.

Such an "inverse promoter effect" was mentioned recently by Olivas et al. who observed that the highly active systems were obtained when the values of R are in the range of 0.8–0.9 and the Ni sulfide particles are surrounded by few layers of WS_2. It was suggested that new active sites appear on the

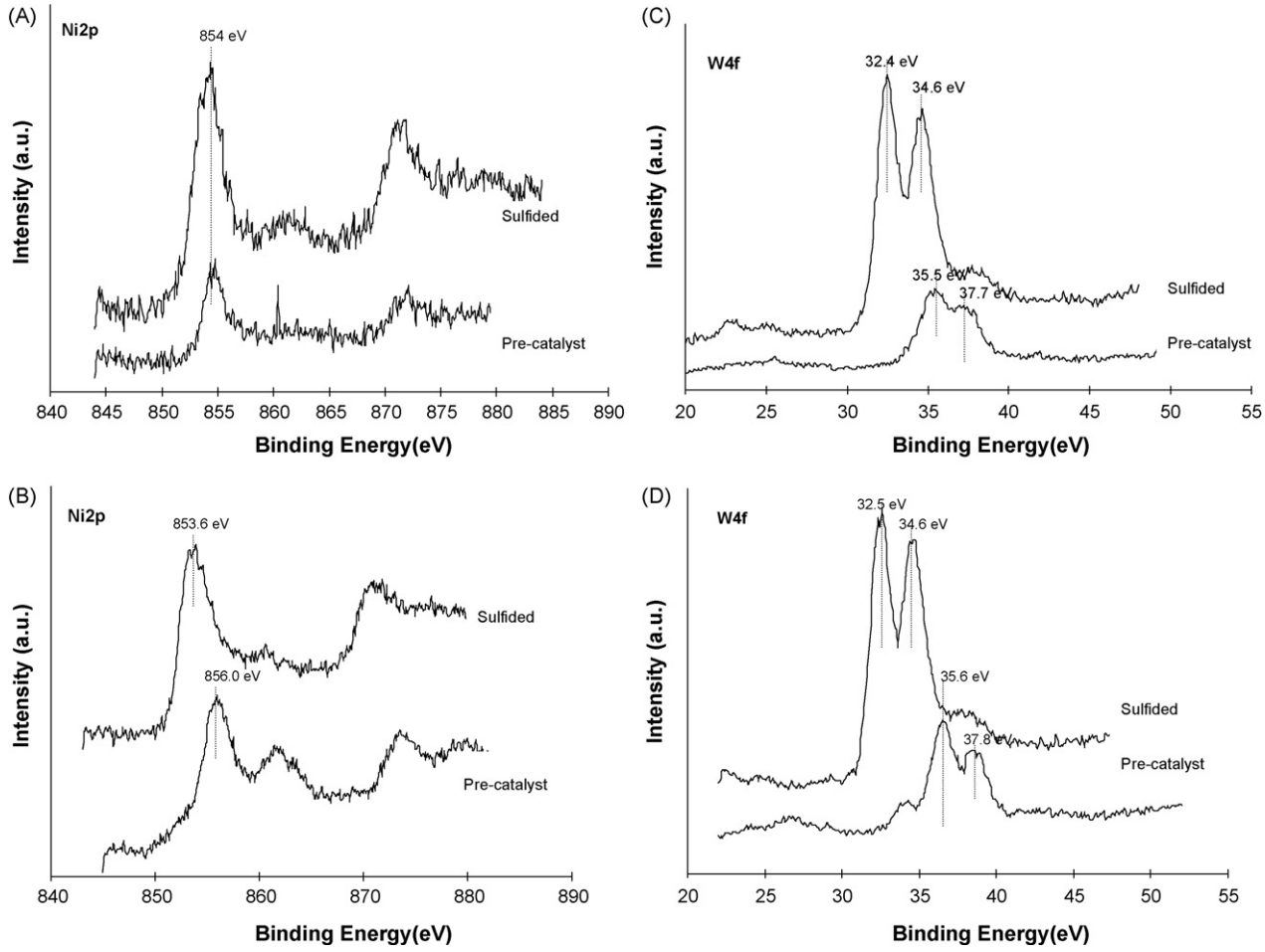

Fig. 4. Ni 2p and W 4f XPS spectra of the pre-catalysts and sulfided NiW catalysts. (A) L_WL_{Ni} Ni 2p, (B) L_WS_{Ni} Ni 2p, (C) L_WL_{Ni} W 4f, (D) L_WS_{Ni} W 4f.

Table 4
XPS binding energies (eV) of elements in the pre-catalysts and sulfided catalysts

Catalysts	S 2p	Ni $2p_{3/2}$		W $4f_{7/2}$	
		Ni–S	Ni–O	W(IV)	W(VI)
L_WL_{Ni} pre-catalyst	162.1–168.9	853.6 (100%)	–	33.1, 35.3 (23%)	35.6, 37.8 (77%)
L_WL_{Ni} sulfided	162.2	854.2 (90%), 853.6 (10%)	–	32.5, 34.6 (81%)	36.0, 38.1 (19%)
L_WS_{Ni} pre-catalyst	162.1–168.8	–	856.0	–	34.6, 36.7 (15%), 35.5, 37.7 (85%)
L_WS_{Ni} sulfided	162.2	853.6 (61%), 854.2 (39%)	–	32.4, 34.6 (84%)	35.8, 38.0 (16%)

curved planes of WS_2. Similar data were observed for the MoS_2 curved slabs [41].

3.3. XPS study

To follow the evolution of surface species, XPS study was carried out comparing the L_WL_{Ni} and S_WL_{Ni} specimens which showed the most striking difference of the properties. The XPS spectra showing Ni 2p levels for two pre-catalysts and the catalysts sulfided at 673 K are presented in Fig. 4 and binding energies of W, Ni and S species are summarized in Table 4. XPS of S 2p on the sulfided NiW/γ-Al_2O_3 catalysts exhibits only one peak at about 162.2 eV, which corresponds to S^{2-} [42,43]. The absence of any signal at 169.0 eV after sulfidation indicates that no oxidation of the catalysts occurred during the transfer of the solid from the sulfiding reactor to the XPS machine. As expected, the intensity of sulfide species peaks increased greatly after sulfidation.

For the L_WL_{Ni} pre-catalyst, a Ni 2p peak could be identified at binding energy of 853.6 eV and attributed to the signal of nickel sulfide phase [6]. After sulfidation, the Ni 2p peaks of L_WL_{Ni} became stronger and the Ni $2p_{3/2}$ binding energy was slightly shifted to the higher energies (854.2 eV). Such a higher binding energy is attributed to the NiWS phase because the Ni atom is a neighbor of the W atom and there is an electronic transfer from Ni to its environment. The situation was quite different for the Ni 2p XPS of the L_WS_{Ni} catalysts. The pre-catalyst L_WS_{Ni} showed a strong Ni 2p peak with the binding energy at 856.0 eV which corresponds to nickel oxide species [8,10]. After sulfidation, the intensity did not change greatly but the Ni 2p peak was shifted to 853.6 eV which is ascribed to formation of nickel sulfide phase. The Ni 2p peak of the L_WS_{Ni} solid was broader than that of L_WL_{Ni} one. The differences of BE allows to suppose that the major part of Ni is in the form of Ni–W–S phase (854.2 eV) for the L_WL_{Ni} solid, whereas it is distributed between NiWS and Ni sulfide in the L_WS_{Ni} one (Table 4).

Deconvolution of the W 4f XPS spectra in our solids revealed the presence of two distinct signals. According to the literature, the BE around 32.4 and 34.6 eV can be ascribed to W(IV) species of WS_2 phase, and the BE around 35.8 and 38.0 eV belong to the signal of W(VI) species [6,22]. After sulfidation, the L_WL_{Ni} and L_WS_{Ni} sulfide catalysts all contained large parts of tungsten sulfide (Fig. 4c and d) but still remained some W(VI) species. As the signal of W(IV) is generally ascribed to WS_2-like species and W(VI) species at BE of 35.8 and 38.0 eV associated to the oxide or oxosulfide species, the percentage of W(IV) can be used to represent the sulfidation degree of W species. It can be seen that the L_WL_{Ni} and L_WS_{Ni} sulfide catalysts had almost the same sulfidation degree of W species: 81 and 84%, respectively. For pre-catalysts, L_WL_{Ni} contained 23% sulfided species, while there are only oxide species in the L_WS_{Ni} one. Combining the results presented above, the pre-catalyst L_WL_{Ni} has higher sulfidation degree of Ni and W species than the pre-catalyst L_WS_{Ni} although there is not much difference after their sulfidation.

In summary, additional insight into the state of tungsten and nickel could be obtained from the XPS data. Difficult sulfidability of tungsten even in the unsupported state has been once more demonstrated. The XPS data evidenced a significant difference of the Ni_{2p} peak binding energy for the two preparations compared. The binding energy of Ni in L_WL_{Ni} catalyst and symmetry of the peak suggest that Ni is mainly incorporated into a NiWS phase. In the L_WS_{Ni} specimen, the Ni_{2p} peak is larger and shifts slightly to lower energy, in agreement with the increase of the part of the Ni sulfide phase coexisting with the NiWS phase.

This behaviour is probably not specific for the bulk catalysts and seems to be common for the supported and unsupported systems. As pointed by Hensen et al. for the supported NiW sulfides [44], low rate of W sulfidation lead to the formation of oxysulfidic tungsten phases (WO_xS_y) if the standard sulfidation conditions are applied. Moreover, the interactions with the alumina support further hinder the W sulfidation degrees. As a result sulfided NiW catalysts supported on alumina or alumosilicates often contain Ni-sulfide particles coexisting with WO_xS_y phases as well as dispersed Ni-sulfide species in 'Ni–W–S'-type phases. Complete transformation of oxysulfide W phases requires increase of sulfidation temperature. At the same time, even when the sulfidation of tungsten was completed, only a part of Ni atoms was incorporated into the Ni–W–S-type phase [44].

4. Conclusions

In this paper we described and compared three new preparations techniques for the Ni–W–S unsupported catalysts. The specific surface areas and catalytic performances reported here are the highest ever observed for the unsupported NiW systems. At the same time we observed high intrinsic activity for the core shell NiS particles covered by curved WS_2 layers. This system had the highest HDS, HYD and HDN activity per unit of surface. Together with earlier works it suggests that the decoration model should be refined for this type of sulfide catalysts.

References

[1] S. Eijsbouts, S.W. Mayo, K. Fujita, Appl. Catal. A 322 (2007) 58.
[2] R. Frety, M. Breysse, M. Lacroix, M. Vrinat, Bull. Soc. Chim. Belg. 93 (1984) 663.
[3] G. Alonso, G. Berhault, A. Aguilar, V. Collins, C. Ornelas, S. Fuentes, R.R. Chianelli, J. Catal. 208 (2002) 359.
[4] L. Jalowiecki, A. Aboulaz, S. Kasztelan, J. Grimblot, J.P. Bonnelle, J. Catal. 120 (1989) 108.
[5] C. Song, A.K. Saini, Energy Fuels 9 (1995) 188.
[6] M. Breysse, M. Cattenot, T. Décamp, R. Frety, C. Gachet, M. Lacroix, C. Leclercq, L. de Mourgues, J.L. Portefaix, M. Vrinat, M. Houari, J. Grimblot, S. Kasztelan, J.P. Bonnelle, S. Housni, J. Bachelier, J.C. Duchet, Catal. Today 4 (1988) 39.
[7] P. Atanasova, T. Tabakova, Ch. Vladov, T. Halachev, A. Lopez Agudo, Appl. Catal. A 161 (1997) 105.
[8] M.J. Vissenberg, Y. van der Meer, E.J.M. Hensen, V.H.J. de Beer, A.M. van der Kraan, R.A. van Santen, J.A.R. van Veen, J. Catal. 198 (2001) 151.
[9] A.J. van der Vlies, G. Kishan, J.W. Niemantsverdriet, R. Prins, Th. Weber, J. Phys. Chem. B 106 (2002) 3449.
[10] A.J. van der Vlies, R. Prins, Th. Weber, J. Phys. Chem. B 106 (2002) 9277.
[11] G. Kishan, L. Coulier, V.H.J. de Beer, J.A.R. van Veen, J.W. Niemantsverdriet, J. Catal. 196 (2000) 180.
[12] H.R. Reinhoudt, A.D. van Langeveld, R. Mariscal, V.H.J. de Beer, J.A.R. Veen, S.T. Sie, J.A. Moulijn, Stud. Surf. Sci. Catal. 106 (1997) 263.
[13] H.R. Reinhoudt, A.D. van Langeveld, R.M. Stockmann, R. Prins, H.W. Zandbergen, J.A. Moulijn, J. Catal. 179 (1998) 443.
[14] B. Scheffer, P.J. Mangnus, J.A. Moulijn, J. Catal. 121 (1990) 18.
[15] J.-C. Duchet, J.-C. Lavalley, S. Housni, D. Ouafi, J. Bachelier, M. Lakhdar, A. Mennour, D. Cornet, Catal. Today 4 (1988) 71.
[16] H.R. Reinhoudt, E. Crezee, A.D. van Langeveld, P.J. Kooyman, J.A.R. van Veen, J.A. Moulijn, J. Catal. 196 (2000) 315.
[17] M.J. Vissenberg, L.J.M. Joosten, M.E.H. Heffels, A.J. van Welsenes, V.H.J. de Beer, R.A. van Santen, J.A.R. van Veen, J. Phys. Chem. B 104 (2000) 8456.
[18] H.R. Reinhoudt, R. Troost, A.D. van Langeveld, J.A.R. van Veen, S.T. Sie, J.A. Moulijn, J. Catal. 203 (2001) 509.
[19] T. Kameoka, H. Yanase, A. Nishijima, T. Sato, Y. Yoshimura, H. Shimada, N. Matsubayashi, Appl. Catal. A 123 (1995) 217.
[20] H. Yasuda, M. Higo, S. Yoshitomi, T. Sato, M. Imamura, H. Matsubayashi, H. Shimada, A. Nishijima, Y. Yoshimura, Catal. Today 39 (1997) 77.
[21] Y. Yoshimura, T. Sato, H. Shimada, N. Matsubayashi, M. Imamura, A. Nishijima, M. Higo, S. Yoshitomi, Catal. Today 29 (1996) 221.
[22] D. Zuo, M. Vrinat, H. Nie, F. Maugé, Y. Shi, M. Lacroix, D. Li, Catal. Today 93–95 (2004) 751.
[23] S. Zeng, J. Blanchard, M. Breysse, Y. Shi, X. Su, H. Nie, D. Li, Appl. Catal. A: Gen. 294 (2005) 59–67.
[24] P. Afanasiev, M. Cattenot, C. Geantet, N. Matsubayashi, K. Sato, S. Shimada, Appl. Catal. A 237 (2002) 227.
[25] Y. Ji, P. Afanasiev, M. Vrinat, W. Li, C. Li, Appl. Catal. A 257 (2004) 157.
[26] Usman, T. Kubota, Y. Okamoto, Bull. Chem. Soc. Jpn. 79 (2006) 637.
[27] R.J.H. Voorhoeve, J.C.M. Stuiver, J. Catal. 23 (1971) 228.
[28] M. Lacroix, M. Vrinat, M. Breysse, Appl. Catal. 21 (1986) 73.
[29] A. Olivas, M. Avalos, S. Fuentes, Mater. Lett. 43 (2000) 1.
[30] J. Espino, L. Alvarez, C. Ornelas, J.L. Rico, S. Fuentes, G. Berhault, G. Alonso, Catal. Lett. 90 (2003) 71.
[31] G. Alonso, J. Espino, G. Berhault, L. Alvarez, J.L. Rico, Appl. Catal. A 266 (2004) 29.
[32] F. Pedraza, S. Fuentes, Catal. Lett. 65 (2000) 107.
[33] A. Olivas, G. Alonso, S. Fuentes, Top. Catal. 39 (2006) 175.
[34] S.P. Kelty, G. Berhault, R.R. Chianelli, Appl. Catal. A 322 (2007) 9.
[35] P. Afanasiev, G.-F. Xia, G. Berhault, B. Jouguet, M. Lacroix, Chem. Mater. 11 (1999) 3216.
[36] D. Genuit, I. Bezverkhyy, P. Afanasiev, J. Solid State Chem. 178 (2005) 2759.
[37] Z. Le, P. Afanasiev, D. Li, Y. Shi, M. Vrinat, C. R. Chimie, in press.
[38] Z. Le, P. Afanasiev, D. Li, X. Long, M. Vrinat, Catal. Comm., in press.
[39] D. Genuit, P. Afanasiev, M. Vrinat, J. Catal. 235 (2005) 302.
[40] R.R. Chianelli, E.B. Prestridge, T.A. Pecoraro, J.P. DeNeufville, Science 203 (1979) 1105.
[41] Y. Iwata, K. Sato, T. Yoneda, Y. Miki, Y. Sugimoto, A. Nishijima, H. Shimada, Catal. Today 45 (1998) 359.
[42] Y. Okamoto, T. Imanaka, S. Teranishi, J. Catal. 65 (1980) 448.
[43] P. Gajardo, A. Mathieux, P. Grange, B. Delmon, Appl. Catal. 3 (1982) 347.
[44] E.J.M. Hensen, Y. van der Meer, J.A.R. van Veen, J.W. Niemantsverdriet, Appl. Catal. A 322 (2007) 16.